
Article:
Pillai, AAS, Anoop, A, Prasad, V et al. (4 more authors) (2018) Multi-proxy evidence for an arid shift in the climate and vegetation of the Banni grasslands of western India during the mid- to late-Holocene. Holocene, 28 (7). pp. 1057-1070. ISSN 0959-6836

https://doi.org/10.1177/0959683618761540

Multi-proxy evidence for an arid shift in the climate and vegetation of the Banni grasslands of western India during the mid to late Holocene

Anusree A S Pillai[1,2,*], Ambili Anoop[3],Vandana Prasad[4], M.C. Manoj[4], Saju Varghese[5], Mahesh Sankaran [1,6], Jayashree Ratnam[1]

Citation:

Pillai AAS, Anoop A, Prasad V, Manoj MC, Varghese S, Sankaran M and Ratnam J (2018) Multi-proxy evidence for an arid shift in the climate and vegetation of the Banni grasslands of western India during the mid to late Holocene, The Holocene. Available at: https://doi.org/10.1177/0959683618761540

Author affiliation and address:

[1] National Centre for Biological Sciences, Tata Institute of Fundamental Research, Bangalore, India.

[2] Manipal University, Madhav Nagar, Manipal 576104, Karnataka, India.

[3] Indian Institute of Science Education and Research Mohali, Manauli, Punjab, 140306, India.

[4] Birbal Sahni Institute of Palaeobotany, Lucknow, India.

[5] Geological Survey of India, Marine and Coastal Survey Division, Salt Lake, Kolkata, 70091, India.

[6] School of Biology, University of Leeds, Leeds LS2 9JT, UK.

*Corresponding author:

National Centre for Biological Sciences, Tata Institute of Fundamental Research, GKVK Campus, Bellary Road, Bangalore, Karnataka 560 065, India. Email: anusreeas@gmail.com

Abstract

Tropical semi-arid grasslands are a widespread and ecologically and economically important terrestrial biome. Here, we use paleoecology to understand woodland-grassland transitions across the mid-to-late Holocene period in the Banni grassland, western India. Multi proxy analyses involving palynology, phytoliths and elemental geochemistry were carried out on two sediment cores retrieved from wetlands (Chachi and Luna), to understand temporal fluctuations in vegetation, moisture availability and other environmental parameters. Based on the results, the Chachi core was divided in to two major climatic phases. Phase 1 (4600–2500 cal yr BP) was characterized by high precipitation and abundance of pollen types and phytolith morphotypes that indicate the presence of woody savanna, and mesic herbaceous taxa. Phase 2 (2500 cal yr BP to the present) was characterized by lower precipitation, lower abundance of mesic taxa and an increase in grass phytolith abundance. However, the period from ~1000 cal yr BP to the present was characterised by the increased abundance of leguminous taxa, dryland herbs/shrubs and a decline in grass phytolith abundance. The Luna core (~1000 cal yr BP to the present) also showed results matching with the Chachi core for this latter period. Overall, moisture availability in the ecosystem appears to have declined since 4600 cal yr BP, and the vegetation has responded to this. Although the balance between tree, shrub and grass elements has fluctuated, overall, the region has remained as an open 'grass and shrub savanna' with sparse woody vegetation throughout this period. Our study

provides insights into the vegetation dynamics and environmental settings in a poorly understood tropical arid-grassland ecosystem from Asia during the mid-late Holocene.

Keywords.

Tropical grassland, mid-late Holocene, geochemistry, pollen, phytolith, palynology, vegetation dynamics.

Introduction

Tropical grassy biomes, which include tropical savannas, woodlands and grasslands, cover nearly 20% of Earth's land surface (Lehmann et al., 2014), support most of the world's livestock, and the livelihoods of nearly a fifth of the world's human population (Olsson and Ouattara, 2013). Despite their recognised importance for human welfare and economy, tropical grassy biomes are amongst the most threatened ecosystems on Earth, and are highly vulnerable to global environmental change and desertification (Sala et al., 2000; Veldman et al., 2015). There is a common and widespread misperception globally, but especially in Asia, that many open grasslands and shrublands are derived from forest clearance or disturbance, and are therefore "degraded" ecosystems (Parr et al., 2014; Bond 2016; Sankaran and Ratnam 2013; Ratnam et al 2016). As a result, they are often the target of afforestation programs or land-use conversions for development (Bond 2016; Ratnam et al. 2016; Veldman 2016). In this context, longer term, historical perspectives of floristic composition and vegetation structure in such regions are essential to distinguish between "natural" and "derived" grasslands (Veldmann, 2016).

The vegetation physiognomy of tropical grassy biomes ranges from open grasslands to dense woodlands, but is characterised by the presence of both these life-forms in the same

landscape (Sankaran et al, 2005; Sankaran and Ratnam, 2013). Globally, the amount and seasonality of rainfall is a primary determinant of the distribution and structure of savannas because it controls plant growth rates, productivity and fire (Williams et al., 1996; Sankaran et al. 2005; Good and Caylor, 2011; Lehmann et al., 2011; Hoffmann et al., 2012; Archibald et al., 2013). However, despite the overarching influence of rainfall in savanna regions with mean annual rainfall <1000 mm globally, the different processes that maintain savannas operate at local and landscape scales, and vary across continents (Staver et al., 2011). A recent comparative study across savannas in Africa, Australia and South America suggests that historical, site-specific differences in climatic regimes and evolutionary histories of species in the different continents likely underlie cross-continental differences in savanna structure and function (Lehmann et al., 2014), suggesting that Asian savannas are also likely to show unique patterns that reflect their distinctive evolutionary and environmental histories.

The results from these studies of contemporary savanna communities highlight the importance of paleoecological studies that trace the histories of vegetation communities over longer time periods in shedding light on our understanding of current day vegetation patterns and dynamics in these ecosystems. Further, paleoecology serves as an important tool to elucidate ecosystem thresholds based on long term vegetation dynamics at different spatial and temporal scales (Willis et al., 2010; Seddon et al., 2015). Recent research from Africa, South America and Australia establishes that in the current geologic epoch, the Holocene, tropical savannas and grasslands have been characterized by large fluctuations in rainfall (Dykoski et al., 2005). Studies also reveal that these ecosystems have shifted between woody and grassy vegetation phases in response to increased or decreased availability of water during the Holocene (Gillson and Ekblom, 2009; Birks et al., 2014; Gliganic et al., 2014). Specifically, the mid to late Holocene period has witnessed reduced precipitation and associated vegetation changes in many of these regions (Birks et al., 2014; Gliganic, 2014).

For instance, paleoecological studies from tropical grasslands in Sahara and Nigeria show that reduced precipitation was the major determinant of vegetation change during the mid-to late Holocene (Waller et al., 2007; Kröpelin et al., 2008).

Paleoclimatic reconstructions of Holocene climates from the arid, semi-arid and sub-humid regions in northwestern India that border the Arabian Sea suggest that the overall intensity of the Indian summer monsoon (ISM) in this region has varied across this epoch (e.g. Prasad et al., 1997; Enzel et al., 1999; Roy et al., 2009; Laskar et al, 2013). This was mainly mediated by the latitudinal shifts in the ITCZ (Inter Tropical Convergence Zone) and ISM changes driven by ENSO (El Niño–Southern Oscillation) and other teleconnections (Haug et al., 2001; Prasad et al., 2014a). Specifically, these regions witnessed periodic incursions of winter precipitation due to the southward shift of westerly winds during the mid-Holocene (Prasad and Enzel, 2006), whereas current day precipitation in this region is dominated by the ISM (Gujarat Institute of Desert Ecology (GUIDE), 1998). Likewise, paleovegetation investigations from these regions show fluctuations in the relative presence of mesic and arid taxa in these regions, corresponding to wet and dry spells until the mid-Holocene (e.g. Singh et al., 1974; Prasad and Enzel, 2006; Prasad et al., 2014b). However, the history of these savanna and grassland ecosystems from the mid-to-late Holocene remains unclear.

Here, we present a new paleoecological record from the Banni grassland-savanna ecosystem of western India, one of the largest savanna-grassland regions in Asia, from the mid-to-late Holocene using multiple proxies including pollen grains, phytoliths and elemental geochemistry. Elemental geochemistry based indices (e.g. Chemical Index of Alteration (CIA) and Chemical Index of Weathering (CIW) and elemental ratios are used to understand weathering conditions and the paleohydrology of the region (Nesbitt and Young, 1982; Harnois, 1988; Arnaud et al., 2012; Brisset et al.,2013). Specifically, we reconstructed the paleovegetational and paleohydrological dynamics of the region based on a multiproxy

investigation of sediment cores from the Banni grassland, with the goal of exploring the nature of linkages between paleovegetation dynamics and paleohydrological regimes of this Asian savanna-grassland ecosystem.

Study area

Location and modern climate

The Banni grassland (23°19' to 23°52' N latitude and 68°56' to 70°32' E longitude; Figure 1(a)) is located south of the marshy salt flats of the Rann of Kachchh in western India and covers an area of nearly 3847 km^2. The region receives an average annual rainfall of ~317 mm with high variability (GUIDE, 1998; Kumar et al., 2015) from the ISM. Mean temperatures in the Banni fluctuate between 49°C in summer (May-June) and 10°C in winter (January-February) (GUIDE, 1998). Currently, the region is characterised by high annual seasonality, recurring drought events and high soil salinity (Kumar et al., 2015).

Geomorphology

The terrain is a flat transitional zone between the rocky uplands of the mainland Kachchh and the Great Rann (Chowksey et al., 2010). Since the Banni is slightly elevated (4 to 20 m above the sea level) from the Great Rann, it is relatively free from marine influences (Patel, 1997). The low elevation and lack of pronounced topographic gradients result in flooding and water logging across large sections of the Banni during the rainy season. The Banni soils are generally fine textured, composed of stratified deposits of silt and clay (Singh and Kar, 2001) resulting in low permeability (Singh and Kar, 2001; Kar, 2011). Soil salinity is highly variable (1.0 to over 15.0 mmhos/cm) and pH ranges between 6.5 and 8.5 (GUIDE, 1998).

The Banni is also characterised by the presence of several anthropogenically undisturbed natural wetlands that provide ideal sites for paleoecological studies.

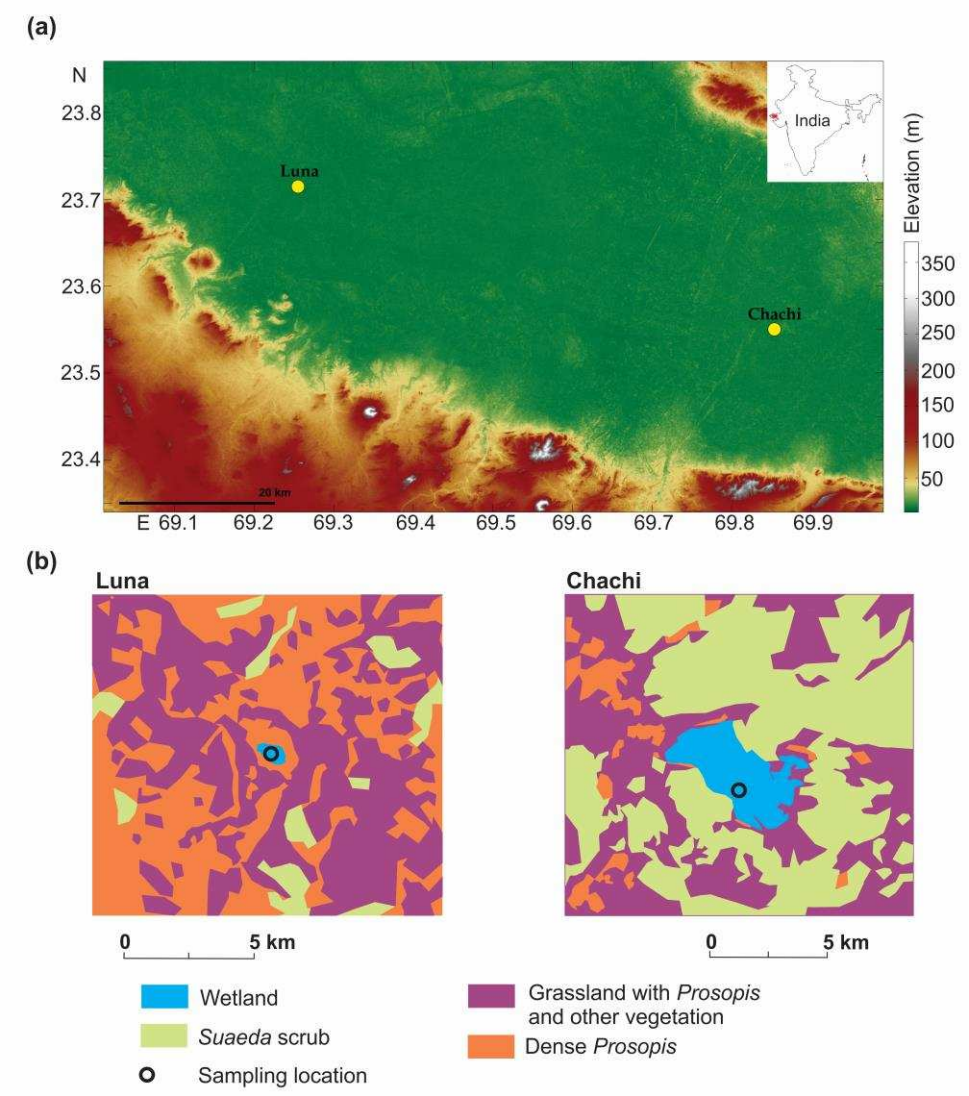

Figure 1 (a) Topography (Luis, 2007) and location of study area (Banni grassland) and sampling sites- Chachi and Luna and (b) vegetation around the wetlands (modified after GUIDE, 2011).

Modern vegetation

Currently, the vegetation in the Banni is a mosaic of open grassland and savanna woodlands (Patel and Joshi, 2011). The region is believed to have supported pastoralism for several centuries (Bharwada and Mahajan, 2012). The understory vegetation is composed of both

salinity tolerant and intolerant herbs (89 species, accounts for ~46% of all the plant species), grasses (37 species, ~19%), shrubs (31 species, ~16%) and trees (17 species, ca. 9%). Climbers and sedges together account for ca. 10% of all plant species (Patel and Joshi, 2011). The ecosystem which sustains nearly 17000 people and >57,000 livestock (GUIDE, 2011), accounts for ~45% of permanent pasture and 10% of grazing land available in Gujarat (Parikh and Reddy, 1997).

Methods

Selection of study sites and sampling

Sediment cores were collected from two sites, viz. the Chachi wetland (23°32'46.788" N and 69°51'9.936" E) towards the eastern Banni and the Luna wetland (23°42'21.3834" N and 69°15'38.268" E) towards the western Banni (Figure 1(a)). These are closed shallow wetlands mainly fed by the ISM runoff. The catchment area of the wetlands is not more than 2 km radius around the wetlands. Sediment cores were raised from the deeper portion of the wetland in summer when they were completely dry.

Chachi, a shallow wetland with an area of ~17.5 km^2 and depth ranging from ~0.5 to 2 m is located in an open landscape composed of Suaeda scrub and grassy vegetation with sparse cover of Prosopis juliflora and other herbaceous vegetation (Figure 1(b)). Sediment samples were collected at 5 cm interval from the walls of a trench up to 70 cm depth followed by coring with a 6 cm diameter PVC pipe from 70 cm up to 142 cm depth, which was in turn subsampled at 4 cm intervals (Figure. 2(a)). Based on the colour and textural variability, the Chachi core was divided in to four zones: 0-74 cm characterised by brown clay with intermittent organic matter layers (i.e., 0-8 cm, 25-45 cm and 60-65 cm), brown silty clay

between 74 cm and 95 cm depths followed by dark brown silty clay until 142 cm depth. There was a band of dark brown silty clay with black clayey patches between 116 cm and 126 cm depth. Mollusc shells were present throughout the Chachi core.

Luna, a shallow wetland with an area of ~0.02 km^2 and depth ranging from 0.5 m in the fringe to ~3 m in the centre is located in a grassland with moderate density of Prosopis juliflora (Figures. 1(b) and 2(b)). Sediment samples were collected at 6 cm intervals first from the walls of a trench up to 60 cm depth and then from a core collected using a PVC pipe of 6 cm diameter up to 85 cm depth. The Luna sediment lithology consists of two major sections: brown silty clay from the surface to 40 cm depth with gastropod shells in the surface layers, followed by brown clay with relatively higher silt content (Figure 2(b)).

Chronology

Chronology was derived using ^{14}C AMS radiocarbon dating of bulk organic matter from four sediment layers of the Chachi core and three layers of the Luna core. Dating was done at the Radiochronology lab in the University of Laval, Canada. The calibration of radiocarbon dates was done according to Reimer et al. (2013) using OxCal 4.2 (Bronk Ramsey, 2008; Bronk Ramsey and Lee, 2013) and the IntCal 13 database (Supplementary Table 1) reported as calibrated years before present (cal yr BP). Age-depth models were developed for the cores by applying linear interpolation to the calibrated ages using the program CLAM 2.2 (Blaauw, 2010) in the R language environment (R Core Team, 2017).

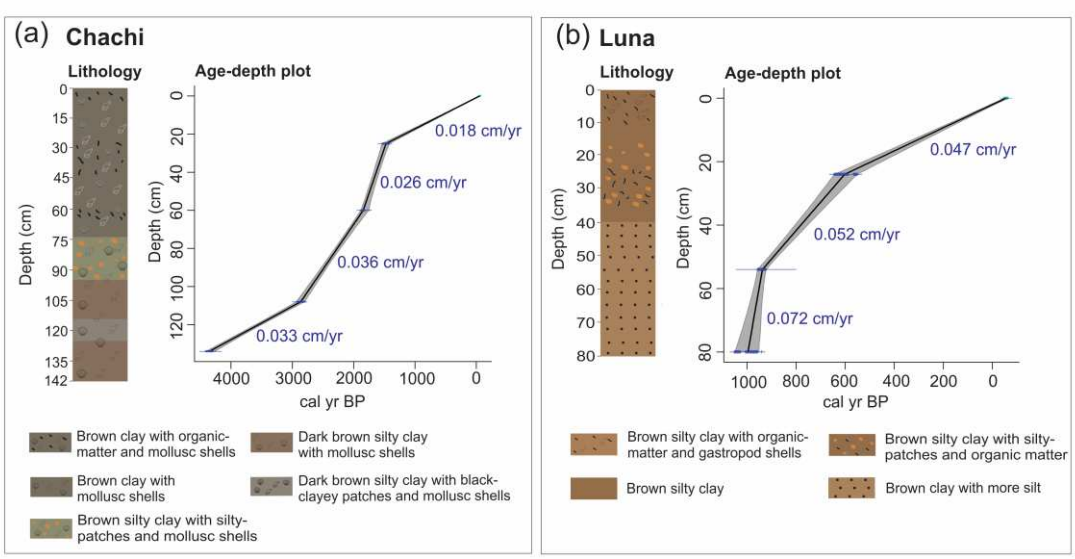

Figure 2. Lithology along with the radiocarbon dates and age-depth plots for Chachi(a) and Luna(b) cores.

Pollen analysis

Sedimentary records of pollen grains have been widely used in paleoecology to understand changes in vegetation composition (Willis et al., 2010) and associated climatic fluctuations (Birks and Birks, 2006). Pollen extraction was carried out following standard protocols (Fægri and Iverson 1989; Bennett and Willis 2001) involving a series of acid treatments (hydrochloric acid (HCl) and hydrofluoric acid (HF)) and acetolysis (a mixture of acetic anhydride and sulphuric acid) (Erdtman, 1943). After chemical extraction, pollen slides were prepared in glycerine jelly and scanned under a compound light microscope (500x). We used rarefaction techniques to estimate the minimum number of pollen grains that had to be counted per sediment layer to account for most of the pollen taxa richness (Birks and Line, 1992; Giesecke et al., 2012). Saturation of pollen richness was reached by 200-300 pollen grains and ~100 pollen grains in the Chachi and Luna cores respectively. We counted 250-300 pollen grains from each sediment layer in the Chachi core (Figure 3(a)), and100 pollen grains for each layer in the Luna core (Figure 3(b)). Exceptions included one layer with low

pollen abundance in the Chachi core, and 3 layers with low pollen abundance in the Luna core.

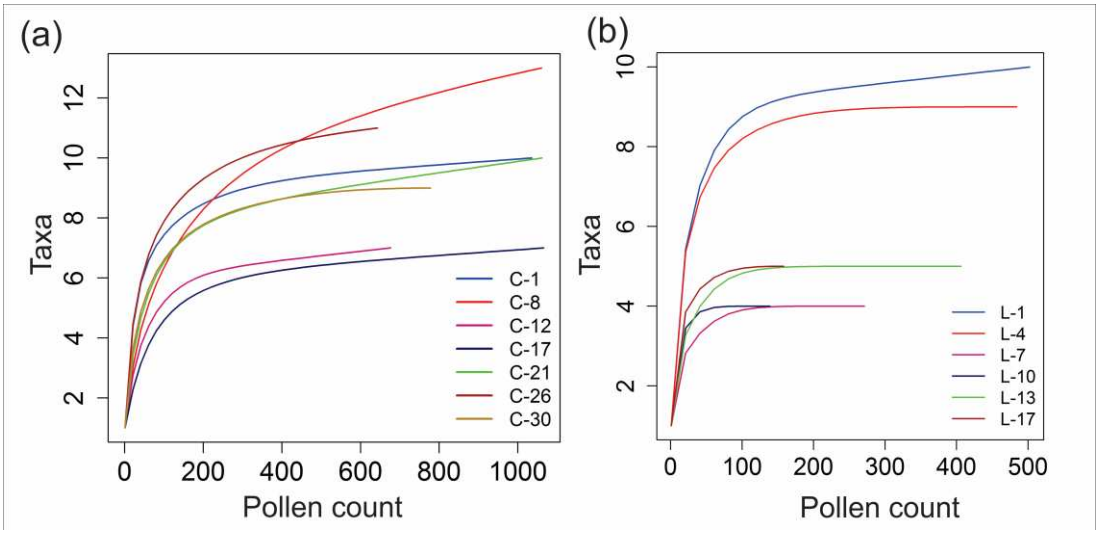

Figure 3. Rarefaction curves at some of the depths for Chachi (a) and Luna (b) cores, representing the minimum number of pollen grains to be counted to account for most of the pollen richness in each sediment layer.

Pollen grains were identified using available pollen databases (Australian Pollen and Spore Atlas, 2007; African Pollen Database, 2000), published literature (Nayar, 1990; Gosling et al., 2013) and pollen reference slides made from the modern vegetation in the Banni. Pollen percentages for each vegetation type were calculated from the relative abundance of pollen types in the respective sediment layers.

The herbaceous/shrub pollen spectra from the Banni region were classified as (i) mesic taxa such as Cyperaceae and Malvaceae that require more moisture for their survival (Gil-Romera et al 2006; Duffin, 2008; Miller and Gosling, 2014), (ii) arid taxa such as Asteraceae, Caryophyllaceae and Euphorbiaceae that require less moisture for their survival (Shmida, 1985; Scott, 1999; Gil-Romera et al 2006; Horn et al, 2014), (iii) taxa that grow in arid and saline conditions such as Chenopodiaceae-Amaranthaceae (Cheno-Ams)(Shmida, 1985; May, 1999; Scott, 1999; Malamud-Roam & Lynn Ingram, 2004; Gil-Romera et al 2006) and (iv) desert taxa such as Ephedra species that grow under arid desert conditions (Singh et al 1974;

Kajale and Deotare, 1997). Arboreal pollen grains included legumes, non-legumes and temperate pines that are wind dispersed.

Phytolith analysis

Phytolith analyses are widely used as reliable indicators of the proportion of grasses versus trees/shrubs in many ecosystems (Stromberg 2004, Piperno, 2006). In the Chachi core, phytoliths were extracted from 10 g of sediments following the heavy-liquid floatation method (Lentfer and Boyd 1998; Piperno 2001). Crushed sediment samples were processed in the following steps: i) removal of carbonates using HCl, ii) oxidation of organic matter by treating with 40% H_2O_2 and subsequent heating, and iii) heavy liquid floatation of phytoliths by centrifugation (1000 rpm for 5 min) of heavy liquid (480 g CdI_2 and 500 g KI in 400 ml distilled water)-sediment mixture (Prasad et al., 2007). In the Luna sediment core layers, which were processed later, phytoliths were analyzed using the microwave digester method (3 ml of HNO_3 and HCl were added to 30 g of crushed sediment and the samples were digested in a microwave sample preparation oven for 30 min; Parr, 2002). Phytoliths were mounted on microscope slides with Canada balsam and scanned under a compound light microscope at 500 x magnification. We counted ~200 phytoliths in most sediment layers.

Phytolith morphotypes were identified (Twiss, 1992; Mulholland and Rapp, 1992; Barboni et al., 1999; Gallego and Distel, 2004; Blinnikov, 2005; Bremond et al., 2005; Lu et al., 2007; Barboni and Bremond, 2009), and classified as either tree, shrub or grass phytoliths (Bremond et al, 2008). Globular phytolith morphotypes are generally derived from trees or shrubs, whereas trapezoid, elongated, fan shaped, saddle, rondel, triangular and ovoid phytolith morphotypes are generally produced by grasses (Mulholland and Rapp, 1992; Twiss, 1992; Bremond et al, 2008). The phytolith morphotypes indicative of different subfamilies of Poaceae were not easily distinguishable in the profile. Therefore, the sum of

all grass phytolith morphotypes in each sediment layer was used for interpretations of the presence of grasses in each layer.

Geochemistry

Major elemental oxides were analysed to understand past environmental conditions of the region (Ankit et al., 2017). Approximately 20 g of air dried sediment sub-samples were desalinized using distilled water before chemical treatment for major element analysis. Samples were crushed in an agate mortar to pass through a -120 +100 ASTM mesh size sieve. The powdered samples were digested with a mixture of concentrated HF–HNO_3–$HClO_4$ following the method of Zhang and Liu, 2002. A fraction (~0.25 gm) from each sub-sample was treated with aqua regia followed by treatment with Hydrofluoric acid (HF) to remove silicates. Perchloric acid was used to remove the organic content in sediments before samples were made up to a 100ml solution using dilute nitric acid. Samples in the nitric medium were fed to a Varian 720-ES Inductively Coupled Plasma Optical Emission Spectrometer (ICP-OES) for major oxide analysis. Based on parallel analyses of international reference materials and in-house standards, major element analytic precision was found to be better than 5%.

Based on elemental geochemistry, we calculated indices and ratios useful for interpreting the paleohydrology of the region. The intensity of alteration/weathering was quantified using the CIA (Nesbitt and Young, 1982) and CIW indices. Chemical weathering alters the composition of siliclastic sediments where larger cations (e.g. Al_2O_3) remain fixed in the weathered residue when compared to smaller cations (e.g. Na, Ca) (Fedo et al 1996; Selvaraj et al., 2004).

CIA was calculated using the formula $CIA = [Al_2O_3/(Al_2O_3 + CaO^* + Na_2O + K_2O)] \times 100$ (Nesbitt and Young, 1982), with CaO* being the amount of CaO incorporated in the silicate

fraction of the rock. The correction to the measured CaO content is necessary to account for the presence of Ca in carbonates and apatites (Fedo et al., 1995). In this study, approximate corrections for CaO were made by assuming reasonable Ca/Na ratios in silicate material content (e.g., McLennan, 1993; Singh et al., 2005). If the CaO molar content is less than that of Na_2O, then the measured CaO content can be used for CaO*; whereas in cases where the CaO molar content is greater than Na_2O, CaO* is assumed to be equivalent to Na_2O (Singh et al., 2005). CIA measures the proportion of Al_2O_3 versus more labile oxides and reflects the relative amount of feldspars and clay minerals in a sample. CIW was calculated using the formula $CIW = [Al_2O_3/(Al_2O_3 + CaO^* + Na_2O)] \times 100$ (Harnois, 1988), with Al_2O_3 treated as an immobile component and CaO* (silicate fraction) and Na_2O used as mobile elements.

The contribution of lithogenic (allochthonous) components depends on the runoff processes that transport sediment particles in the catchment (Konig et al., 2003; Whitlock et al., 2012; Shanahan et al., 2013). Intense precipitation results in a large supply of terrigenous materials into the wetland (Peng et al., 2005; Anoop et al., 2013). Anthropogenically induced erosion also contributes to increased terrigenous flux (Brisset et al., 2013; Bhattacharya et al., 2015). These elemental concentrations show distinct behaviors under different climatic conditions. During periods of high precipitation, terrigenous materials are washed into wetlands resulting in increased concentrations of Al_2O_3, TiO_2 and Fe_2O. All these elements are relatively mobile, and tend to migrate in the aqueous form. Under wet weather conditions, clay minerals retain K^+ and Mg^{2+} in preference to Na^+ or Ca^{2+} (Nesbitt et al., 1980; Nesbitt and Young, 1996). Mg and K are thus less influenced by weathering, and concentrated as a result of lower mobility (Nesbitt et al., 1980). This is also evident from weathering intensity parameters such as CIA, CIW and elemental indices (Nesbitt et al., 1980; Nesbitt and Young, 1996; Tao et al., 2006; Minyuk et al., 2007, 2011). Based on the geochemical behavior of the major elements, the following indices– CaO/TiO_2, CaO/MgO, Na_2O/TiO_2 and Fe_2O_3/TiO_2

can be used to infer changes in environmental conditions of the study area. Lower values of Na_2O/TiO_2 and CaO/TiO_2 and increased values of Fe_2O_3/TiO_2 reflect increased precipitation (Muhs et al., 2001; Sinha et al., 2006; Kotlia and Joshi, 2013), while higher CIA values associated with lower values of CaO/MgO indicate a warm and wet climate (Sun et al., 2010).

Data analysis

The sums of grass and tree phytoliths were plotted as time series, and trend components based on five point moving averages were estimated for each time-series using the "TTR" library (Ulrich, 2016) in the statistical package R (R Core Team, 2017).

We performed Principal Component Analysis (PCA) on pollen, phytolith and elemental concentrations of the Chachi core profile. All data were standardized before running the analysis. PCA was done to estimate the association between parameters (Loska and Wiechula, 2003) and to reduce the dimensionality of the dataset so as to identify time segments that represent similar proxy values. PCA extracts the main variation in the dataset by linear combinations of the original data and generates a new set of uncorrelated variables called Principal Components (PCs). PCA was carried out using the 'stats' package in R statistical program (R Core Team, 2017). Further, PCA Axis One values were plotted against their corresponding ages.

Results

Chronology of the sediments

The ^{14}C AMS dates from both Chachi and Luna cores were stratigraphically consistent.

Linear interpolation shows that the Chachi core spans ca.4600 cal yr BP and Luna core spans

ca. 997 cal yr BP (Pillai et al., 2017). The sedimentation rate in the Chachi profile was 0.037 cm/yr from ~3300 to 2000 cal yr BP, followed by a gradual decline towards the present (0.018 cm/yr) (Figure 2(a)). The sedimentation rate in the Luna profile was 0.08 cm/yr at ~1000 cal yr BP, which gradually declined to 0.040 cm/yr by ~603 cal yr BP, followed by a gradual increase towards the present (0.055 cm/yr) (Figure 2(b)).

Chachi sediment profile

More than 90% of the pollen counted from the Chachi core were herbaceous/shrub pollen, whereas arboreal pollen grains were not abundant, particularly in the upper parts of the sediment core. The most frequently occurring herbaceous taxa in the Chachi core were Cyperaceae, Malvaceae, Asteraceae, Caryophyllaceae, Euphorbiaceae, Chenopodiaceae-Amaranthaceae (Cheno-Ams) type and Ephedra (Figure 4; Supplementary Figure 1). Cheno-Ams was the most dominant pollen type across all depths. Ephedra pollen fluctuated across the core from 4600 to 1000 cal yr BP, followed by an increasing trend towards the present. Amongst arboreal pollen, Pinaceae pollen were more abundant before ca. 3000 cal yr BP, Syzygium pollen was present only in certain depths between 4600 and 2000 cal yr BP, Combretaceae pollen was present ca.4600 cal yr BP and in certain depths between 2000 and 500 cal yr BP and leguminous arboreal pollen (including pollen from native Acacia and Prosopis species, and the more recently, introduced exotic Prosopis juliflora) were present at certain depths ~4600 cal yr BP and 3500 cal yr BP, and in all depths from ~2000 cal yr BP towards the present.

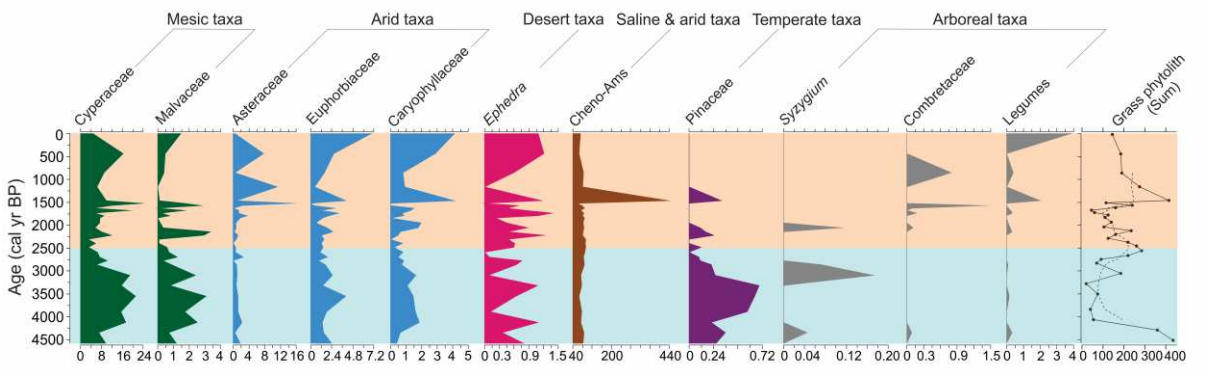

Figure 4. Pollen diagram of the Chachi core (C2 Version 1.4.3). Percentages of frequently occurring pollen types and grass phytolith abundance in the Chachi core are plotted against ages of different sediment layers.

Grass phytolith morphotypes (trapezoid, elongated, fan shaped, saddle, rondel, triangular, ovoid etc.; see Supplementary Figure 2) were present throughout the Chachi and Luna cores. These were more abundant in Chachi core from 4600 to 4200 cal yr BP, 2800 to 2000 cal yr BP and 1500 to 1000 cal yr BP and in the Luna core between 1000 to 600 cal yr BP. Tree/shrub phytolith morphotypes (globular) were present in the sediment layers only before 3500 cal yr BP in Chachi profile, but were present throughout the Luna profile (Figure 5).

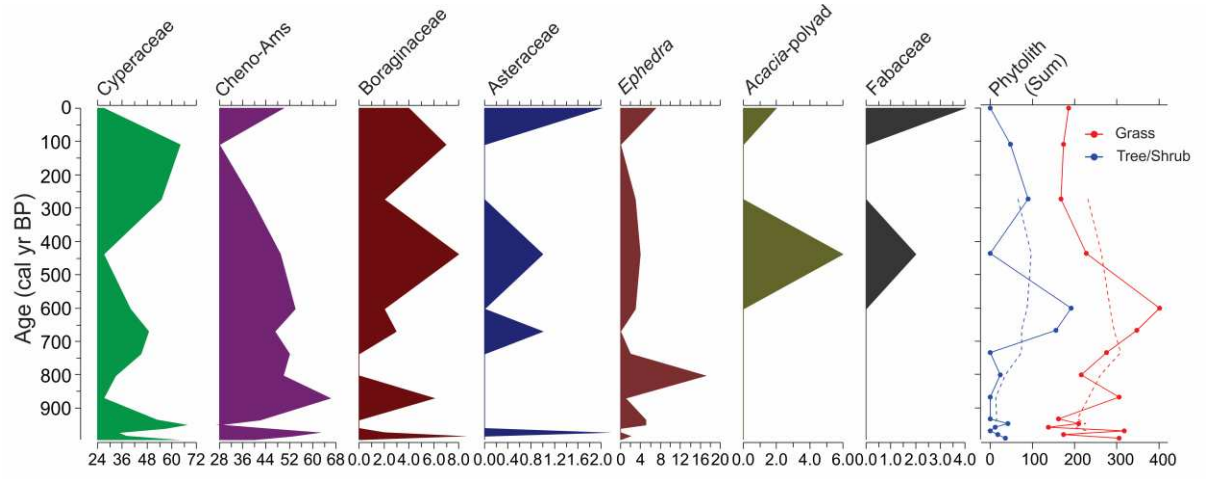

Figure 5. Pollen diagram of the Luna core (C2 Version 1.4.3). The percentages of frequently occurring pollen types and grass and tree/shrub phytolith abundances in the Luna core across different depths plotted against ages of sediment layers. Dashed lines in phytolith plots represent trend lines based on five-point moving average filters.

The distribution of the major element oxides along the age profile is shown in Figure 6. The elements TiO_2 and Fe_2O_3 showed similar patterns and were significantly correlated with

Al_2O_3 (r = 0.60, and 0.92 respectively) for the Chachi record. The Al_2O_3 concentration in the Chachi core sediments fluctuated between 17.57–22.9% (average = 20.79%). Concentration of the other major oxides like Fe_2O_3, TiO_2, MgO, CaO, Na_2O, K_2O and MnO_2 varied between 11.1–16.45%, 0.95–1.2%, 3.18–3.93%, 3.63–8.37%, 0.98–2.06, 2.81–3.86% and 0.05–0.09%, respectively. Downcore variations in CaO concentrations showed a weak negative correlation (r = –0.32) with Al_2O_3 in the Chachi core sediments. This weak correlation may be the result of Ca being derived from dual sources: authigenic calcium carbonate (e.g. $CaCO_3$ shells present in the core) and calcium bearing detrital minerals.

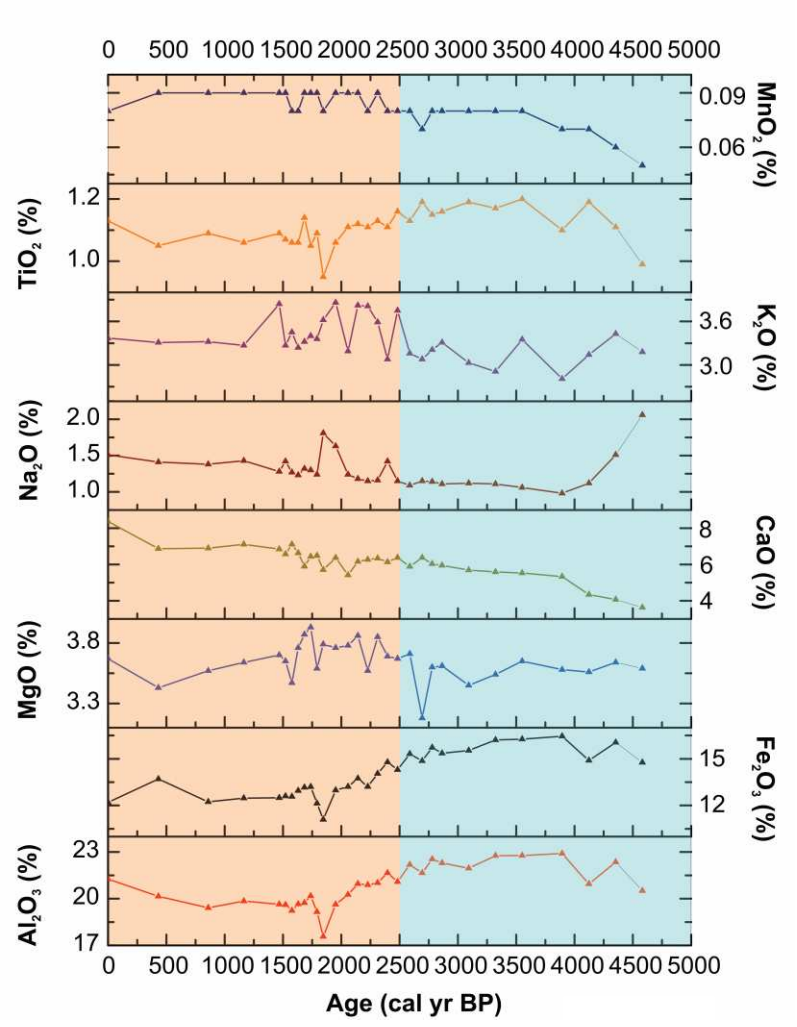

Figure 6. Concentrations of major elements in Chachi core are plotted across age.

The first two axes of the PCA ordination (PC1 and PC2) based on selected pollen types, grass phytoliths and geochemical proxies in the Chachi core explained 27% and 17%, respectively, of the variation in the dataset. PCA axes 1 and 2 separated the 142 cm long Chachi profile into two zones based on vegetation type and geochemical proxies: the shallower, more recent sections of the Chachi profile (~2500 cal yr BP to the present) and the deeper layers (~4600 cal yr BP to ~2500 cal yr BP) (Figure 7a and 7b). PC1 was positively associated with variables - Na_2O, K_2O, MgO, CaO, Cheno-Ams, grass phytolith, Ephedra, Asteraceae, Caryophyllaceae etc. and negatively correlated with Fe_2O_3, Al_2O_3, TiO_2, and Malvaceae and Cyperaceae pollen. PC2 was positively correlated with Euphorbiaceae, Caryophyllaceae, Ephedra and Cheno-Ams pollen and negative associated with Asteraceae pollen and Na_2O. Based on PCA analysis, Chachi profile was divided in to two time zones.

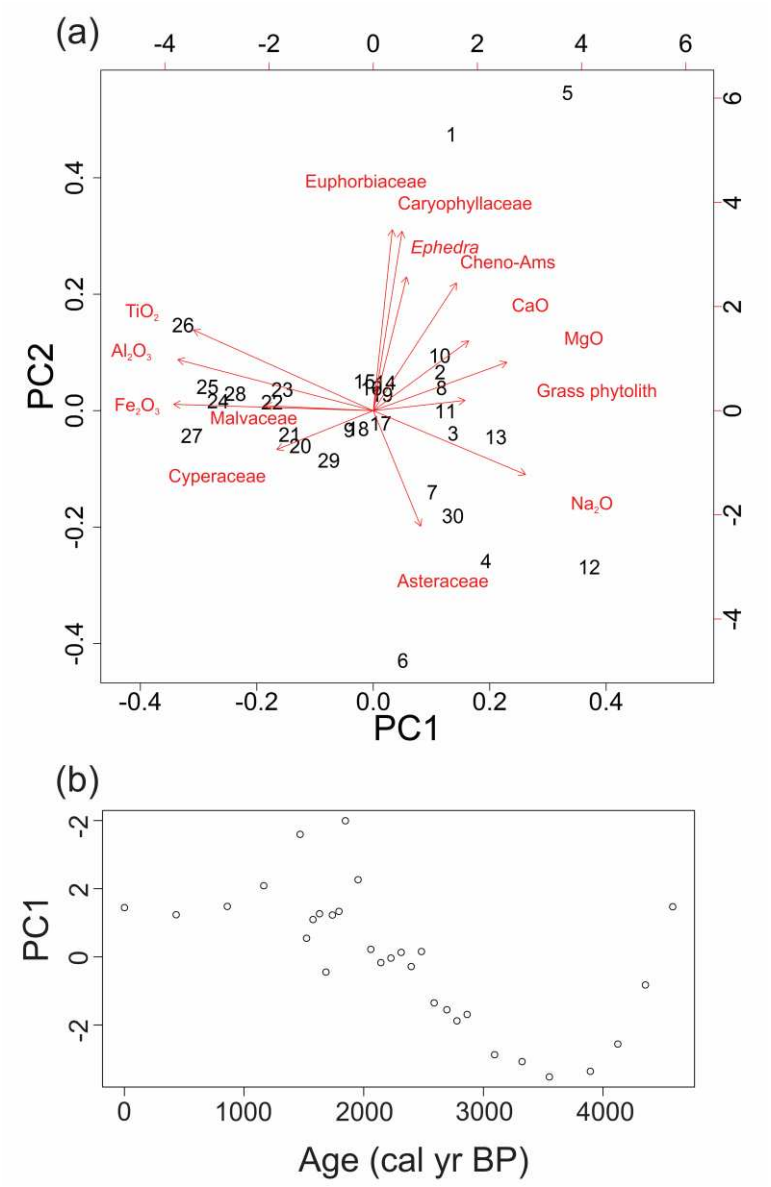

Figure7. (a) PCA biplot based on principal component analysis of proxies in Chachi core and (b) Principal component axis one (PC1) plotted against age. The numbers in plot (a) represent depth profiles of the sediment cores, with 1 being the shallowest and 30 the deepest.

Zone 1 (142 to 90cm depth) ~4600–2500 cal yr BP.

This zone was marked by a high abundance of herb/shrub taxa including Cyperaceae and Malvaceae, a low abundance of Asteraceae, Euphorbiaceae and Caryophyllaceae and the presence of arboreal taxa such as Prosopis, Combretaceae and Syzygium ca.4200 cal yr BP, and Acacia and Syzygium between 3441–2862 cal yr BP (Figure 4). Phytolith recoveries in

this zone indicated a high abundance of grass phytolith morphotypes both towards the beginning and end of this zone (Figure 4).

Geochemical analyses revealed low values of Al_2O_3, Fe_2O_3 and TiO_2 between 4600-4000 cal yr BP followed by a period of high values (ca.4000-3000 cal yr BP). CaO, K_2O and MnO_2 showed very low values from 4600–2500 cal yr BP. Na_2O showed the highest concentration between 4000–4600 cal yr BP, while MgO did not show much variation in this zone (Figure 6).

Zone 2 (90cm depth to surface) ~2500 cal yr BP to the present.

The beginning of this zone (~2500 to ~2200 cal yr BP) was characterised by the decreased abundance of some herbaceous taxa including Cyperaceae and Malvaceae, and increased or unchanged abundance, relative to the previous zone, of others such as Asteraceae and Euphorbiaceae. Arboreal pollen of Prosopis, Combretaceae, Syzygium and Acacia were absent during this time, while Pinaceae pollen decreased in abundance (Figure 4). Grass phytolith morphotypes showed an increase in abundance at the beginning of this zone (Figure 4). Al_2O_3 concentration across this period mirrored mesic taxa, with a declining trend relative to Zone 1 (Figure 6).

There was a slight increase in the abundance of herbaceous taxa, Cyperaceae and Malvaceae from ~2200 to 2000 cal yr BP and from 1700 to 1500 cal yr BP and after ~1000 cal yr BP towards the present. Arboreal pollen of Prosopis, Combretaceae, Syzygium and Acacia appeared again ~2133 to 1951 cal yr BP. After this, Syzygium pollen grains were not found in the sediments. Between ~2000 -1700 cal yr BP and 1500-1000 cal yr BP, there was a decline in the abundance of herbaceous taxa– Cyperaceae and Malvaceae. The pollen types - Asteraceae, Caryophyllaceae, Euphorbiaceae and Ephedra gradually increased after ~2500 cal yr BP and then declined between ~1200 cal yr BP and ~950 cal yr BP, after which they

increased to very high values towards the present (Figure 4). The dominant pollen taxa Cheno-Ams showed a peak between ~1500 and ~1200 cal yr BP, followed by a decline and then a consistent abundance towards the present. Leguminous trees increased in abundance from ~ 600 cal yr BP to the present (Figure 4). Grass phytolith morphotypes declined gradually between 2200 cal yr BP and 1800 cal yr BP, and then increased again until ~1000 cal yr BP, after which they gradually declined and remained relatively low and constant towards the present (Figure 4).

Al_2O_3, Fe_2O_3 and TiO_2 showed gradual decreases during this period from ca.2500–1000 cal yr BP, and their lowest values are reported in the period between 2000 and 1700 cal yr BP. In contrast, the concentrations of other major oxides like MgO, CaO, Na_2O, K_2O and MnO_2 were relatively higher than in the previous zone, althought they fluctuated considerably between ~2500 and 1500 cal yr BP (Figure 6). Al_2O_3 showed relatively low values till ca.1000 cal yr BP followed by slightly increased concentrations thereafter. The period after ~1500 cal yr BP was characterised by relatively constant values of MgO, CaO, Na_2O, K_2O and MnO_2 (Figure 6).

Luna sediment profile:

The Luna sediment pollen profile, which covers a shorter time period towards the late Holocene (~1000 cal yr BP to present) was composed mainly of the herb/shrub pollen taxa such as Cyperaceae, Cheno-Ams, Boraginaceae, Asteraceae and Ephedra, that increased in abundance towards the present, albeit with some intermediate fluctuations. Leguminous tree pollen of Acacia and Prosopis were also present after ~600 cal yr BP and increased in abundance towards the present (Figure 5).

Phytolith morphotypes of grasses and trees/shrubs were present through the Luna profile. From ~1000 cal yr BP until ~600 cal yr BP, there was an increase in abundances of grass

phytolith morphotypes, after which it declined in abundance. Tree/shrub phytolith morphotypes were low between ~1000 and 600 cal yr BP and after ~500 cal yr BP towards the present, but showed a peak between 600 and 500 cal yr BP (Figure 5).

Discussion

Paleo-environment and vegetation changes from Banni sediments

Reconstructions of past vegetation and environmental conditions based on wetland sediment cores indicate the prevalence of open grasslands with sparse woody vegetation during the mid to late Holocene in the Banni. However, our results also indicate a mesic to arid shift in vegetation during this period corresponding to climatic and weathering conditions, supported by both pollen and geochemical proxies. These mesic periods were also associated with increased weathering conditions, which we interpret as mediated by increased Indian Summer Monsoon (ISM) precipitation. These results are further supported by precipitation reconstructions for the region based on oxygen isotope indicators (Pillai et al., 2017). Our results indicate that the period from 4600 cal yr BP to 2500 cal yr BP was characterized by wet conditions with high abundance of arboreal taxa such as Syzygium. In contrast, the period from ~2500 cal yr BP to the present is characterised by relatively lower weathering conditions, and greater representation of arboreal taxa characteristic of Asian and African savannas, including Combretaceae and Acacia species. Our results also indicate a shift in dominance from broad-leaved (Combreatceae) to fine-leaved (Acacia) arboreal species in the last 500 years, and an increase in the abundance of many arid taxa (Figure 4).

Zone 1(~4600–2500 cal yr BP)– a period of high moisture availability

This period is characterised by pollen of mesic and arboreal taxa (Figure 4) and tree/shrub phytolith morphotypes (~4600 to 3500 cal yr BP) that are suggestive of high moisture availability. These data suggest that the Chachi catchment area was relatively mesic during the mid-late Holocene transition period (ca.4600 cal yr BP to 2500 cal yr BP). However, the mesic pollen taxa gradually started to decline from ~3000 cal yr BP. Likewise, Combretum and Syzygium species and Malvaceae in contemporary African savannas are found in regions with more than 600 mm/yr rainfall (White, 1983; Olson et al., 2001; Miller and Gosling, 2014). This period in the current study was also marked by the presence of Pinaceae pollen, a temperate taxa brought in to the landscape by wind. Pinaceae pollen morphology supports long distance wind dispersal and these pollen in the profile may have come during times of stronger winds in the landscape (Figure 4). Increased grass phytolith abundance between ~4600-4200 cal yr BP and from ~3000 cal yr BP to ~2500 cal yr BP coincided with the lower abundance of mesic pollen taxa, which could be due to the relatively arid conditions during this time. (Figure 4).

Geochemical parameters also reflect what is seen in the pollen and phytolith data. High values of Al_2O_3, Fe_2O_3, TiO_2, Fe_2O_3/TiO_2, CIA and CIW suggest intense chemical weathering and erosion in the catchment (Figures 6 and 8). Lower CaO/TiO_2 and CaO/MgO also suggest higher precipitation and warmer-wetter conditions (Figure 8).

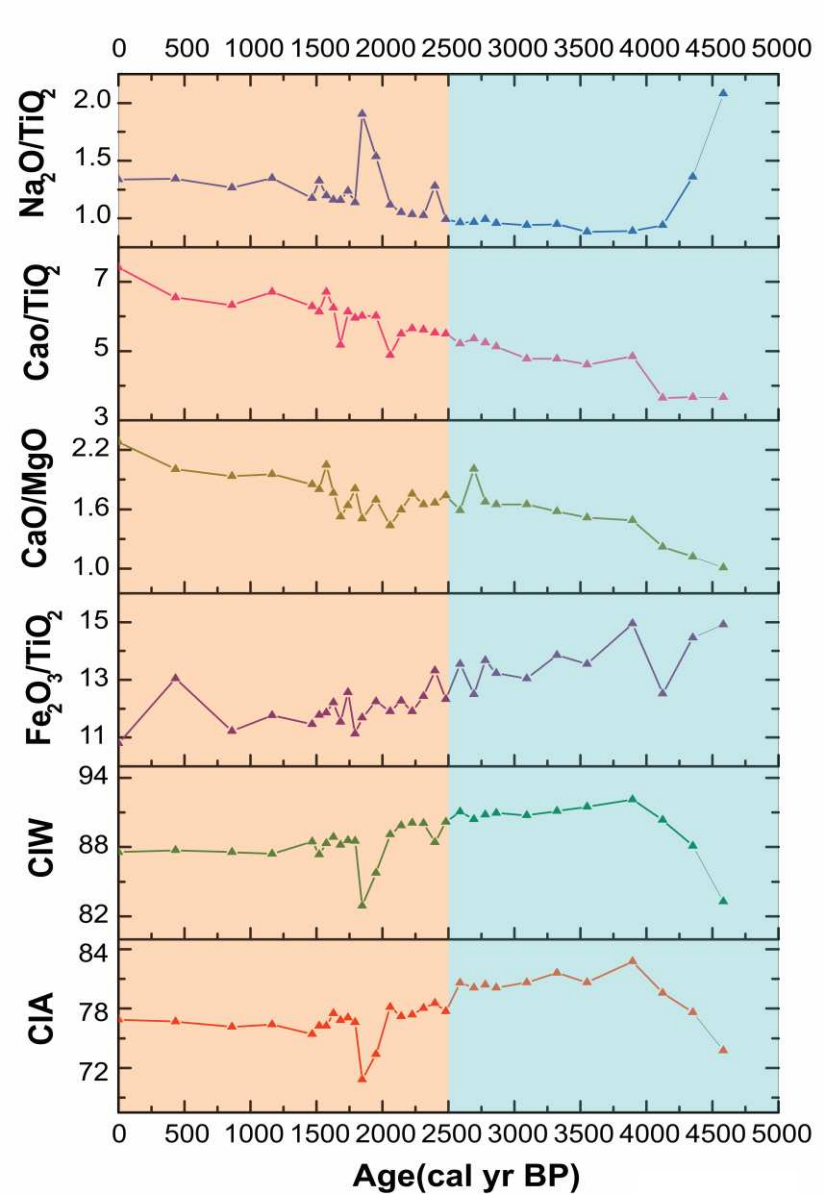

Figure 8. CIA, CIW and other geochemical indices in Chachi core are plotted across age.

CIA: Chemical index of alteration; CIW: Chemical index of weathering.

Zone 2(~2500 cal yr BP to the present)– a period of declining precipitation.

This phase is characterised by an overall decline in precipitation. However, there were several intermediate fluctuations during this phase, with a slight increase in moisture availability from ~1000 cal yr BP towards the present. The abundance of mesic herbaceous taxa remained low during ~2500 to ~1000 cal yr BP with some intermediate fluctuations.

However, pollen that are representative of arid climate did not show clear declines during this period. Higher grass phytolith abundance in this phase relative to the previous phase can be attributed to increased arid conditions, while periods of lower grass phytolith abundance from ~2000 to ~1600 cal yr BP, and the slight decline after ~1000 cal yr BP following a peak at ~1200 cal yr BP (Figure 4) may be due to both climatic and disturbance factors (Pillai et al., 2017). The period from ~1000 cal yr BP towards the present is marked by an increase in all other herbaceous taxa (Figure 4). This may have been caused by shifts in disturbance regimes such as fire and herbivory (Pillai et al., 2017) coupled with climatic factors. Evidence from contemporary studies suggests that changes in fire regimes and intense grazing by cattle can allow shrubs and herbs to replace C_4 grasses and encroach onto savannas (Roques et al., 2001; Eldridge et al., 2011). Increased moisture availability can further accelerate shrub encroachment (O'Connor 1995), while drought conditions can reduce shrub abundances by imposing heavy mortality (Rouques et al., 2001). In the Banni, an increase in the abundance of leguminous tree pollen taxa from around 600 cal yr BP towards the present may be due to both climatic and edaphic conditions in the region. Acacia and Prosopis are common arid tree genera in the Mimosoideae sub-family of Leguminosae and are capable of withstanding drought and saline conditions (Munzbergova and Ward, 2002; Felker, 2009; Sprent, 2009).

Decreasing values of Al_2O_3, Fe_2O_3, TiO_2, Fe_2O_3/TiO_2, CIA and CIW and higher values of CaO/TiO_2, CaO/MgO, Na_2O/TiO_2, Na_2O and CaO (Figures 6 and 8) in the Chachi core reflect weaker hydrodynamics, poor chemical weathering, slower erosion and are suggestive of reduced rainfall under semiarid to arid climatic conditions during this phase. However, the period from ~ 500 cal yr BP towards the present shows slightly increased values of Al_2O_3 and TiO_2 which likely reflect increased regional precipitation and thus stronger chemical weathering (Figure 6). The time periods from ~2200 to 2000 cal yr BP and ca.1700–1500 cal

yr BP also show slight increases in mesic taxa, CIA, CIW and other indicators suggestive of relatively higher precipitation (Figures 4, 6 and 8).

The Luna catchment area remained as open grassland characterised by grassy vegetation and also other herbaceous and shrub taxa from ~1000 cal yr BP towards the present. The increased abundance of herbaceous taxa and leguminous tree taxa coinciding with a decline in grass phytolith abundance (Figure 5) may also be due to the cumulative effect of climatic factors and biotic disturbances as in the case of the Chachi sediment profile.

Plant distributions are often governed by a combination of broad-scale bioclimatic and historic factors as well as the local conditions at a particular site (Barbour et al., 1987). Our results suggest that while regional climatic factors influenced broad-scale patterns of vegetation composition and changes across this landscape, vegetation composition also varied across catchments in response to local-scale differences in micro-climate and habitat parameters. The two wetlands (Chachi and Luna) separated by a distance of ~70 km, show variations in edaphic properties and micro-habitats. But the reconstructed climatic variability across both the sediment profiles shows similar patterns of change through the late Holocene (Pillai et al., 2017). The sites also show comparable trends of increases in herbaceous taxa and disturbance tolerant leguminous taxa towards the present. Thus, while broad scale biotic/abiotic drivers were reflected across both sites, minute fluctuations were not equally captured in both the profiles, likely due to site specific changes in sediment accumulation rates.

Regional comparison of paleo-environment and vegetation reconstruction

Vegetation and geochemical signals indicate that the period from ca. 4600-2800 cal yr BP was relatively mesic in the Banni. Other pollen studies conducted across the arid and semi-arid zones of Rajasthan also suggest that the period between ~4600 to ~3000 cal yr BP was

marked by an increase in tree and shrub vegetation including genera Syzygium, Mimosa, Acacia, Prosopis, Capparis, Tamarix etc. (Singh et al., in 1974). Likewise, this mesic phase and subsequent arid phase have been reported from palynological and geochemical records from the currently arid (Singh et al., 1974; Swain et al., 1983; Roy et al., 2009), semi-arid and sub-humid ISM belts of western India (Laskar et al., 2013; Prasad et al., 2014b). A recent multi-proxy study from the semi-arid region of Saurashtra coast in northwest India also suggests a relatively humid climate and higher sea-level between 4710 and 2825 cal yr BP followed by a gradual onset of aridity between 2825 and 1835 cal yr BP (Banerji et al., 2015). A dry spell is also recorded between ~2300 and 1100 cal yr BP in another record from the arid belt in Western India (Roy et al., 2009). These signals are found in the Chachi core with the prevalence of an arid phase during 2500–1700 cal yr BP, associated with a decline in mesic herbaceous taxa and a decline in weathering indices. A high resolution pollen, biomarker and isotope record from central India indicates drought conditions between ~2000 and 600 cal yr BP (Prasad et al., 2014a). In the Chachi core, a relatively wet interval is observed between 1700 and 1500 cal yr BP with the reappearance of all the arboreal pollen taxa and a decline in the abundance of grass phytoliths. Likewise, slightly wet events are captured in the geochemistry and palynological records from the Sourashtra coast from ~1800 to ~1500 cal yr BP (Banerji et al., 2015).

Other terrestrial records from regions receiving ISM rainfall also show similar patterns in mid-late Holocene rainfall change. For instance, geochemical records from Eastern India also show increased precipitation between 4600 and 3100 cal yr BP followed by a reduction in monsoonal strength towards the present (Ankit et al., 2017). Studies based on palynology and $\delta^{18}O_{carb}$ values from western and northwest Himalayas also show a progressive decrease in precipitation and (I/E) ratios ((meltwater + monsoon precipitation)/evaporation) during the mid-late Holocene (Leipe et al., 2014; Mishra et al., 2015; Demske et al., 2016; Figure 9).

Isotopic records from northeast Himalaya also show a shift towards arid conditions from ~2700 cal yr BP to ~1300 cal yr BP (Agrawal et al., 2015). Several marine and terrestrial records explaining ISM variability show millennial-scale climate fluctuations during the Holocene, with drier conditions from ~2500 to ~1500 cal yr BP and ~1000 to 650-450 cal yr BP from different regions (Patnaik et al., 2012).

Several well dated records of paleoclimate variability from the Arabian Sea suggest an increase in aridity after the mid Holocene associated with a weakening of the summer monsoon winds (Naidu, 1996; Lückge et al., 2001; Gupta et al., 2003). A high resolution record from the northeastern Arabian Sea off Pakistan showed increased aridity from ~3000 cal yr BP to ~2000 cal yr BP, followed by a period of enhanced summer monsoon rainfall until ~1500 cal yr BP (Lückge et al., 2001). Another record from the Arabian Sea near the Oman margin shows several abrupt fluctuations in the Asian southwest monsoon during the mid-late Holocene and an overall trend of gradual decline in rainfall after ~4600 cal yr BP to the present (Gupta et al., 2003).

In the Banni, the period between 1500 to 600 cal yr BP experienced relatively arid climate with more grassy vegetation and arid taxa. There was an increase in pollen abundance of Ephedra and arid taxa, but also of legumes and some mesic taxa. From ~1200 cal yr BP to the present, there was a decrease in grass phytoliths. These trends cannot be attributed only to the slight increase in precipitation, but may have also been influenced by multiple environmental factors acting on the ecosystem. The slight increase in precipitation since ~600 cal yr BP as shown by the geochemical data is associated with an increase in the abundance of herb/shrub taxa in the pollen records. This may have been due to changes in biotic disturbance regimes (Pillai et al., 2017) and other human mediated processes acting on the ecosystem. Records from the arid, semi-arid belt in western India suggest that a mix of C_3 and C_4 vegetation during the late Holocene shifted to more C_3 vegetation towards the present

(Laskar et al., 2013). Likewise, a record from the semi-arid region in the central India also suggests an increase in C_3 isotopic signal and in herbaceous pollen records from ~1200 cal yr BP to the present (Prasad et al., 2014a). These recent increases in C_3 signals are attributed to anthropogenic activities replacing grasses with herb and woody taxa (Laskar et al., 2013, Prasad et al., 2014a).

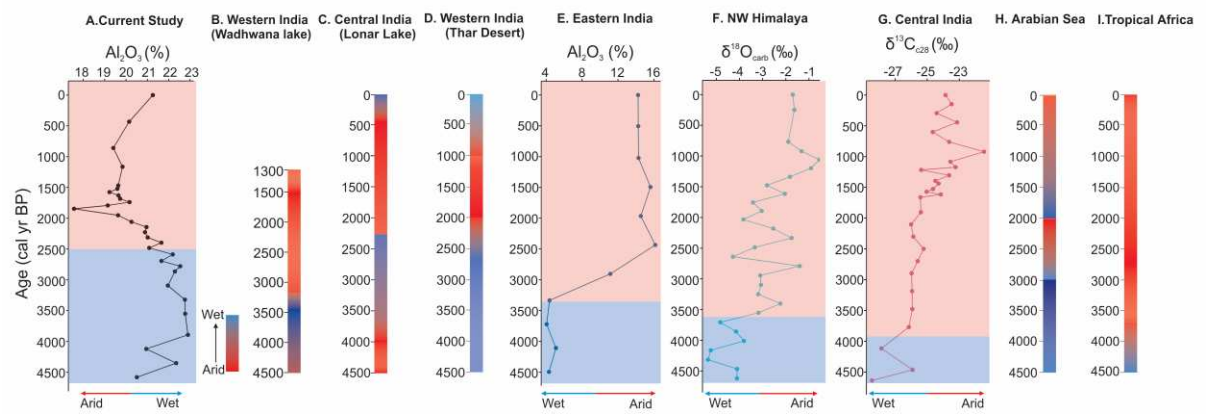

Figure 9. Spatio-temporal comparison of Banni climate data with other paleoclimate records: (a). Al_2O_3 (%)of Chachi-core (present study); (b). palynology, phytolith and carbon isotope data from Wadhwana Lake in the semi-arid region of mainland Gujarat, western India (Prasad et al., 2014b); (c). presence of evaporite minerals in Lonar lake, central India (Anoop et al., 2013; Prasad et al., 2014a); (d). geochemical signature from Thar Desert, western India (Roy et al, 2009); (e). Al_2O_3 (wt%) from continental shelf sediments near Rushikulya river, eastern India (Ankit et al. 2017); (f). $\delta^{18}O_{carb}$ data from Tso Moriri Lake, northwest Himalayas (Mishra et al., 2015); (g). carbon isotope data from biomarkers derived from the Godavari catchment (Ponton et al., 2012); (h). geochemical evidence from northeastern Arabian sea (Lückge et al, 2001) (i). palynological, geochemical and other paleoenvironmental records from tropical Africa (Kröpelin et al., 2008; Waller et al., 2007).

The mesic period in the Chachi core during ~4600 cal yr BP to ~2800 cal yr BP also matches trends reported from the tropics and sub-tropics of Africa and other regions of Asia. Increased precipitation in parts of tropical Africa and the greening of Sahara and Sahel have been documented during the mid-Holocene (Gasse, 2000), alongside increased lake levels throughout East Africa (Verschuren et al., 2009; Tierney et al., 2011; Berke et al., 2012) and West-central Africa (Schefuß et al., 2005; Shanahan et al., 2006). Multiple records from the tropics and sub-tropics in Asia also suggest the presence of increased precipitation during the

mid-Holocene (Singh et al., 1974; Swain et al., 1983; Roy et al., 2009; Laskar et al., 2013; Prasad et al, 2014b; Figure 9). As in the case of the Banni records, arid conditions occurred progressively after the mid to late Holocene in north and western Africa (Kröpelin et al., 2008; Waller et al., 2007). Studies from the northwestern Arabian sea, Peninsular India and Himalayan regions demonstrate the beginning of aridity by around 4000–3500 cal yr BP (Gupta et al., 2003; Staubwasser et al., 2003; Caratini et al., 1994; Phadtare, 2000; Prasad et al., 2014b). Studies from the northern sub-tropics suggest that there was an abrupt decline in the intensity of Asian monsoon by around 3500 cal yr BP (Dykoski et al., 2005). The mesic period was followed by a noticeable weakening of summer monsoon in Africa and Asia resulted in the increasing aridity of these regions due to the progressive southward shift of northern hemisphere summer positions of Intertropical Convergence Zone (ITCZ) (Gasse, 2000; Wanner et al., 2008). Similar to the recorded slight increase in precipitation in Banni sediment from 600 cal yr BP to the present, equatorial east Africa remained humid during 600–150 cal yr BP (Verschuren et al., 2000), which may be due to more complex mechanisms than the classic "cool poles, dry tropics" pattern (Mayewski et al., 2004).

The mid-late Holocene weakening of summer monsoon in the current study can be explained by the weakening of summer monsoon caused by southward latitudinal shift in the annual mean position of ITCZ and orbitally forced reduction in solar insolation (Haug et al., 2001). This affected precipitation across the tropics in the northern hemisphere by causing an increase in ISM precipitation in regions closer to the equator and a reduction in precipitation in regions near the northern transition zone of ISM domain (Fleitmann et al., 2007). Apart from this, ENSO has been reported as a significant climatic forcing controlling the variability of ISM precipitation (Kumar et al., 1999; Prasad et al., 2014a). ENSO events associated with the warmest sea surface temperature (SST) anomalies in the central equatorial Pacific have been reported to cause significant reductions in ISM rainfall (Kumar et al., 2006). Several

independent studies suggest that the frequency of ENSO events increased after the mid-Holocene (Haug et al., 2001; Moy et al., 2002; Rein et al., 2005), with associated increases in arid conditions and climatic variability during the mid-late Holocene (Haug et al., 2001). In the current study, arid conditions associated with frequent fluctuations in the climate records during ~2800 to ~1500 cal yr BP may be a coupled effect of changes in ENSO and solar insolation.

Conclusions

This study shows that the Banni region remained a 'grass and shrub savanna' throughout the mid- late Holocene with some compositional shifts captured mainly by temporal fluctuations in the relative abundances of grass, woody, mesic and arid taxa. Variations in the geochemical compositions of the sediments, mediated mainly by chemical weathering indicate increased rainfall in the region during mid-Holocene (~4600–2500 cal yr BP), which then gradually decreased towards the present. Shifts in vegetation composition broadly match that of rainfall, with more woody taxa during mid-Holocene from ~4600–2500 cal yr BP, more grassy vegetation and arid herbaceous taxa during ~2500 to 1200 cal yr BP and followed by a gradual decrease in grassy vegetation, fluctuations in arid and mesic herbaceous taxa and increases in leguminous woody taxa, especially form ~600 cal yr BP to the present. Overall, vegetation responses to precipitation change were most prominent during the mid-late Holocene transition period (~4600–2800 cal yr BP). The pronounced fluctuations in the vegetation composition of key taxa during the late-Holocene (~2500 cal yr BP to the present), rather than being in response to rainfall alone, may also have been in response to edaphic factors like salinity and human use of the landscape for herbivory and charcoal. The recent increases in drought-tolerant leguminous woody taxa and herbaceous taxa in the landscape are also likely to be due to factors other than rainfall. At the present

time, a major vegetation change in the ecosystem is the spread of an introduced, invasive species (Prosopis juiflora) and the cascade of events associated with this; this spread is driven by a combination of anthropogenic and climatic factors. Thus, changes in the recent past and present are likely driven by cumulative effects of climatic, landscape and anthropogenic factors; it will be important to disentangle these for the future management of this ecosystem.

Acknowledgements

We thank everyone who have helped during the field work including Banni field staff, staff in Sahjeevan and faculty from the Department of Earth and Environment Science, Kachchh University and Mr. Sujith B.S. We are also grateful to the infrastructure and logistical support provided by the National Centre for Biological Sciences, TIFR and Birbal Sahni Institute of Palaeobotany, Lucknow, India.

Funding

This research was supported by research grants from Ravi Sankaran Foundation (http://www.ravisankaran.org/the-fellowship/fellowships/), Research and Monitoring in the Banni Landscape Grant (RAMBLE - http://www.bannigrassland.org/), Jawaharlal Nehru Memorial Fund (JNMF - http://www.jnmf.in/sabout.html) and French Institute of Pondicherry (IFP) Local doctoral scholarship (BL) Sep-Oct 2012 (http://ifpindia.org/) to PAAS and core funding from the National centre for Biological Sciences (NCBS - https://www.ncbs.res.in/) to MS.

Author contributions:

AASP, JR, MS and AA conceptualized the study. Sediment core and field data collection was carried out by AASP. Analysis and interpretetation of pollen and phytolith data was carried

out by AASP and VP, and geochemistry data by AA, SV and MMC. AASP drafted the manuscript with significant contributions from JR. JR, MS, AA and VP provided critical feedback on the manuscript.

References

Agrawal S, Srivastava P, Meena NK et al. (2015) Stable isotopes and magnetic susceptibility record of late Holocene climate change from a lake profile of the Northeast Himalaya. Journal of Geological Society of India 86(6): 696–705.

Ankit Y, Kumar P, Anoop A et al. (2017) Mid-late Holocene climate variability in the Indian monsoon: evidence from continental shelf sediments adjacent to Rushikulya river, eastern India. Quaternary International 443: 155-163.

Anoop A, Prasad S, Plessen B et al. (2013) Palaeoenvironmental implications of evaporative Gaylussite crystals from Lonar lake, Central India. Journal of Quaternary. Science 28(4): 349–359.

APSA Members (2007) The Australasian Pollen and Spore Atlas V1.0. Australian National University, Canberra. Available at: http://apsa.anu.edu.au/ (accessed 17 July 2014).

Archibald S, Lehmann CER, Gómez-dans JL and Bradstock RA (2013) Defining pyromes and global syndromes of fire regimes. Procedings of National Academy of Science U S A. 110(16): 6445-6447.

Arnaud F, Révillon S, Debret M et al. (2012) Lake Bourget regional erosion patterns reconstruction reveals Holocene NW European Alps soil evolution and paleohydrology. Quaternary Science Reviews 51: 81–92.

Banerji US, Pandey S, Bhushan R and Juyal N (2015) Mid-Holocene climate and land-sea interaction along the southern coast of Saurashtra, western India. Journal of Asian Earth Sciences 111: 428-439.

Barboni D and Bremond L (2009) Phytoliths of East African grasses: An assessment of their environmental and taxonomic significance based on floristic data. Review of Palaeobotany and Palynology 158(1-2): 29-41.

Barboni D, Bonnefille R, Alexandre A and Meunier JD (1999). Phytoliths as paleoenvironmental indicators, West Side Middle Awash Valley, Ethiopia. Palaeogeography, Palaeoclimatology, Palaeoecology 152(1-2): 87–100.

Barbour MG, Burk JH and Pitts WD (1987) Terrestrial Plant Ecology, 2nd ed. Melno Park: Benjamin Cummings Publishing Co.

Bennett KD. and Willis KJ (2001). Pollen. In: Smol JP, Birks HJB and Last WM (eds.). Tracking Environmental Change Using Lake Sediments. Volume 3: Terrestrial, Algal, and Siliceous Indicators. The Netherlands: Kluwer Academic Publishers, pp. 5-32.

Berke MA, Johnson TC, Werne JP et al. (2012) Molecular records of climate variability and vegetation response since the Late Pleistocene in the Lake Victoria basin, East Africa. Quaternary Science Review 55: 59-74.

Bharwada C and Mahajan V (2012). Let it be Banni- Understanding and sustaining pastoral livelihoods of Banni. CESS monograph 26, RULNR monograph – 13, Centre for Economic and social studies, Begumpet, Hyderanbad.

Bhattacharya T and Byrne R (2016) Cultural implications of late Holocene climate change in the Cuenca Oriental, Mexico. Proceedings of the National Academy of Sciences 112(6): 56-69.

Birks HH and Birks HJB (2006) Multi-proxy studies in palaeolimnology. Vegetation History and Archaeobotany. 15(4): 235-251.

Birks HJB and Line JM (1992). The use of rarefaction analysis for estimating palynological richness from Quaternary pollen-analytical data. The Holocene 2(1):1–10.

Birks J, Mackay A and Oldfield F (2014). Global change in the Holocene. New York: Routledge.

Blaauw M (2010) Methods and code for 'classical' age-modelling of radiocarbon sequences. Quaternary Geochronology 5(5): 512–518.

Blinnikov MS (2005) Phytoliths in plants and soils of the interior Pacific Northwest, USA. Review of Palaeobotany and Palynology 135(1-2): 71–98.

Bond WJ (2016) Ancient grasslands at risk. Science 351(6269): 120–122.

Bremond L, Alexandre A, Hély C and Guiot J (2005) A phytolith index as a proxy of tree cover density in tropical areas: Calibration with Leaf Area Index along a forest-savanna transect in southeastern Cameroon. Global and Planetary Change 45(4): 277–293.

Bremond L, Alexandre A, Wooller MJ et al. (2008) Phytolith indices as proxies of grass subfamilies on East African tropical mountains. Global and Planetary Change 61(3-4):209–224.

Brisset E, Miramont C, Guiter F et al. (2013) Non-reversible geosystem destabilisation at 4200 cal. BP: Sedimentological, geochemical and botanical markers of soil erosion recorded in a Mediterranean alpine lake. The Holocene 23(12): 1863–1874.

Bronk Ramsey C (2008). Deposition models for chronological records. Quaternary Science Review 27(1-2): 42-60.

Bronk Ramsey C and Lee S (2013). Recent and Planned Developments of the Program OxCal. Radiocarbon 55(2-3): 720-730.

Caratini C, Bentaleb I, Fontune M et al. (1994) A less humid climate since ca. 3500 yr BP from marine cores off Karwar, western India. Palaeogeography, Palaeoclimatology, Palaeoecology 109 (2–4): 371–384.

Chowksey V, Maurya DM, Khonde N and Chamyal LS (2010). Tectonic geomorphology and evidence for active tilting of the Bela, Khadir and Bhanjada islands in the seismically active Kachchh palaeorift graben, Western India. Zeitschrift für Geomorphologie 54(4): 467–490.

Demske D, Tarasov PE, Leipe C et al. (2016). Record of vegetation, climate change, human impact and retting of hemp in Garhwal Himalaya (India) during the past 4600 years. The Holocene 26(10): 1-15.

Duffin KI (2008) The representation of rainfall and fire intensity in fossil pollen and charcoal records from a South African savanna. Review of Palaeobotany and Palynology 151(1-2): 59–71.

Dykoski CA, Edwards RL, Cheng H et al. (2005) A high resolution, absolute dated Holocene and deglacial Asian monsoon record from Dongge Cave, China. Earth and Planetary Science Letters 233(1-2): 71-86.

Eldridge DJ, Bowker MA, Maestre FT, Roger E, Reynolds JF, Whitford WG (2011) Impacts of shrub encroachment on ecosystem structure and functioning: towards a global synthesis: synthesizing shrub encroachment effects. Ecology Letters 14(7): 709–722.

Enzel Y, Ely L, Mishra, S et al (1999) High-Resolution Holocene Environmental Changes in the Thar Desert, Northwestern India. Science 284(5411):125–128.

Erdtman G (1943) An Introduction to Pollen Analysis. Waltham Mass, Chronica Botanica Co.

Fægri K and Iversen J (1989). Text book of pollen Analysis. 4th Edition. Blackburn Press.

Fedo CM, Eriksson K, Krogstad EJ (1996). Geochemistry of shales from the Archean Abitibi greenstone belt, Canada: Implications for provenance and source-area weathering. Geochimica et Cosmochimica Acta 60: 1751–1763.

Fedo CM, Nesbitt HW, Young, GM (1995). Unravelling the effects of potassium metasomatism in sedimentary rocks and paleosols, with implications for paleoweathering conditions and provenance. Geology 23(10): 921–924.

Felker P (2009) Unusual physiological properties of the arid adapted tree legume Prosopis and their applications in developing countries. In: Barrera ED and Smith WK (eds) Perspectives in Biophysical Plant Ecophysiology: A Tribute to Park S. Nobel, Mexico: Universidad Nacional Autonoma de Mexico, pp. 221–255.

Fleitmann D, Burns SJ, Mangini A, Mudelsee M, Kramers J, Villa I, et al. (2007) Holocene ITCZ and Indian monsoon dynamics recorded in stalagmites from Oman and Yemen (Socotra). Quaternary Science Review 26(1-2):170-188.

Gallego L and Distel RA (2004) Phytolith assemblages in grasses native to central Argentina. Annals of Botany 94(6): 865–874.

Gasse F (2000) Hydrological changes in the African tropics since the Last Glacial Maximum. Quaternary Science Review 19(1-5): 189–211.

Giesecke T, Wolters S, Jahns S and Brande A (2012). Exploring Holocene Changes in Palynological Richness in Northern Europe - Did Postglacial Immigration Matter? PLoS ONE 7(12), 51624.

Gillson L and Ekblom A (2009) Resilience and thresholds in savannas: Nitrogen and fire as drivers and responders of vegetation transition. Ecosystems, 12(7): 1189-1203.

Gil-Romera G, Scott L, Marais E and Brook GA (2006) Middle- to late-Holocene moisture changes in the desert of northwest Namibia derived from fossil hyrax dung pollen. The Holocene 16(8): 1073–1084.

Gliganic LA, Cohen TJ, May J-H et al. (2014) Late-Holocene climatic variability indicated by three natural archives in arid southern Australia. The Holocene 24(1):104-117.

Good SP and Caylor KK (2011) Climatological determinants of woody cover in Africa. Proceedings of the National Academy of Sciences108(12): 4902–4907.

Gosling WD, Miller CS and Livingstone DA (2013). Atlas of the tropical West African pollen flora. Review of Palaeobotany and Palynology 199: 1–135.

Gujarat Institute of Desert Ecology (GUIDE) (1998) Status of Banni Grassland and Exigency of Restoration Efforts. Report, Gujarat Ecology Commission, Vadodara, Gujarat.

Gujarat Institute of Desert Ecology (GUIDE) (2011) An integrated grassland development in Banni, Kachchh District, Gujarat State. Annual Progress Report 2010-2011, Gujarat Department of Forest and Environment (GDFE), Gandinagar.

Gupta AK, Anderson DM, Overpeck JT (2003). Abrupt changes in the Asian southwest monsoon during the Holocene and their links to the North Atlantic Ocean. Nature 421: 354–357.

Harnois L (1988) The CIW index: a new chemical index of weathering. Sedimentary Geology 55(3-4): 31–32.

Haug GH, Hughen KA, Sigman DM et al. (2001) Southward migration of the intertropical convergence zone through the Holocene. Science 293(5533): 1304–1308.

Hoffmann WA, Jaconis SY, Mckinley KL et al. (2012) Fuels or microclimate? Understanding the drivers of fire feedbacks at savanna-forest boundaries. Austral Ecology 2012;37(6):634-643.

Horn JW, Xi Z, Riina R et al. (2014) Evolutionary bursts in Euphorbia (Euphorbiaceae) are linked with photosynthetic pathway. Evolution, 68(12): 3485–3504.

Kajale MD and Deotare BC (1997) Late Quaternary environmental studies on salt lakes in western Rajasthan, India: a summarised view. Journal of Quaternary Science 12(5): 405-412.

Kar A (2011) Geomorphology of the Arid Lands of Kachchh and its Importance in Land Resources Planning. In: Bandyopadhyay S, Bhattacharji M, Chaudhuri S, Goswami D Jog SR and Kar A (eds). Landforms Processes & Environment Management. Kolkata: ACB Publications. Pp. 388-414.

Konig KA, Shotyk W, Lotter AF et al. (2003). 9000 years of geochemical evolution of lithogenic major and trace elements in the sediment of an alpine lake - the role of climate, vegetation and land/use history. Journal of Paleolimnology 30(3): 307-320.

Kotlia BS and Joshi LM (2013) Late holocene climatic changes in Garhwal Himalaya. Current Science 104(7): 911–919.

Kröpelin S, Verschuren D, Lézine A-M et al. (2008) Climate-driven ecosystem succession in the Sahara: the past 6000 years. Science 320(5877):765-768.

Kumar KK, Rajagopalan B and Cane MA (1999) On the Weakening Relationship Between the Indian Monsoon and ENSO. Science 287(5423): 2156–2159.

Kumar KK, Rajagopalan B, Hoerling M, Bates G and Cane M 2006. Unraveling the mystery of Indian monsoon failure during El Niño. Science 314(5796), 115–119.

Kumar VV, Mahato AKR, Patel R (2015) Ecology and Managenet of Banni grasslands of Kachchh, Gujarat. In: Rawat GS and Adhikari BS (eds) Ecology and Management of Grassland Habitats in India, ENVIS Bulletin. Wildlife & Protected Areas, Wildlife Institute of India, Dehradun Vol. 17: 240 pp.

Laskar AH, Yadava MG, Sharma N and Ramesh R (2013) Late-Holocene climate in the Lower Narmada valley, Gujarat, western India, inferred using sedimentary carbon and oxygen isotope ratios. The Holocene 23(8): 1115–1122.

Lehmann CER, Anderson TM, Sankaran M et al. (2014) Savanna vegetation-fire-climate relationships differ among continents. Science 343(6170): 548-552.

Lehmann CER, Archibald SA, Hoffmann, WA and Bond, WJ (2011) Deciphering the distribution of the savanna biome. New Phytologist, 191(1), 197–209.

Leipe C, Demske D, Tarasov PE et al. (2014) A Holocene pollen record from the northwestern Himalayan lake Tso Moriri: implications for palaeoclimatic and archaeological research. Quaternary International 348: 93-112.

Lentfer CJ and Boyd WE (1998) A Comparison of Three Methods for the Extraction of Phytoliths from Sediments. Journal of Archaeological Science 25(12): 1159-1183.

Loska K and Wiechuła D (2003) Application of principal component analysis for the estimation of source of heavy metal contamination in surface sediments from the Rybnik Reservoir. Chemosphere 51(8): 723-733.

Lu H, Wu N, Liu K et al. (2007) Phytoliths as quantitative indicators for the reconstruction of past environmental conditions in China II: palaeoenvironmental reconstruction in the Loess Plateau, Quaternary Science Reviews 26(5-6): 759-772.

Lückge A, Doose-Rlinski H, Khan AA et al. (2001). Monsoonal variability in the northeastern Arabian Sea during the past 5000 years: geochemical evidence from laminated sediments. Palaeogeography,Palaeoclimatology, Palaeoecology 167, 273–286.

Luis JF (2007) Mirone: A multi-purpose tool for exploring grid data. Computers & Geosciences. 33: 31-41.

Malamud-Roam F and Lynn Ingram B (2004) Late Holocene d13C and pollen records of paleosalinity from tidal marshes in the San Francisco Bay estuary, California. Quaternary Research 62(2): 134-145.

Mayewski PA, Rohling EE, Stager JC et al. (2004) Holocene climate variability. Quaternary Research 62(3): 243-255.

May MD (1999) Vegetation and salinity changes over the last 2000 years at two islands in the northern San Francisco Estuary, California. MA Thesis, University of California, Berkeley.

McLennan SM (1993) Weathering and global denudation. Journal of Geology 101(2): 295–303.

Miller CS and Gosling WD (2014) Quaternary forest associations in lowland tropical West Africa. Quaternary Science Reviews 84(15): 7–25.

Minyuk PS, Borkhodoev VYa and Goryachev NA (2011) Geochemical Characteristics of Sediments from Lake El'gygytgyn, Chukotka Peninsula, as Indicators of Climatic Variations for the Past 350 ka, Doklady Earth Sciences 436(1): 94–97.

Minyuk PS, Brigham-Grette J, Melles M et al. (2007) Inorganic geochemistry of El'gygytgyn Lake sediments (northeastern Russia) as an indicator of paleoclimatic change for the last 250 kyr. Journal of Paleolimnology 37(1): 123–133.

Mishra PK, Prasad S, Anoop A et al. (2015) Carbonate isotopes from high altitude Tso Moriri Lake (NW Himalayas) provide clues to late glacial and Holocene moisture source and atmospheric circulation changes. Palaeogeography, Palaeoclimatology, Palaeoecology 425: 76–83.

Moy CM, Seltzer GO, Rodbell DT and Anderson DM (2002) Variability of El Nin˜o/Southern oscillation activity at millennial time- scales during the Holocene epoch. Nature 420: 162–165.

Mühs DR, Bettis, EA, Been J and McGeehin JP (2001) Impact of climate and parent material on chemical weathering in loess derived soils of the Mississippi river valley. Soil Science Society of America Journal 65; 1761–1777.

Mulholland SC and Rapp G Jr (1992) A morphological classification of grass silica-bodies. In: Rapp G Jr and Mulholland SC (eds) Phytolith Systematics: Advances in archaeological and Museum Science. New York: Plenum Press, pp. 65–89.

Munzbergova Z and Ward D (2002) Acacia trees as keystone species in Negev desert ecosystems. Journal of Vegetation Science 13(2): 227–236.

Naidu PD (1996). Onset of an arid climate at 3.5 ka in the tropics: evidence from monsoon upwelling record. Current Science 71 (9): 715–718.

Nayar TS (1990) Pollen flora of Maharashtra state. Mumbai:Today & Tomorrows Printers and Publishers.

Nesbitt HW and Young GM (1982) Early Proterozoic climates and plate motions inferred from major element chemistry of Lutites. Nature 299: 715–717.

Nesbitt HW and Young GM (1996) Petrogenesis of sediments in the absence of chemical weathering: effects of abrasion and sorting on bulk composition and mineralogy. Sedimentology 43(2): 341-358.

Nesbitt HW, Markovics G and Price RC (1980) Chemical processes affecting alkalis and alkali earths during continental weathering. Geochimica et Cosmochimica Acta 44: 1659–1666.

O'Connor TG (1995) Acacia karroo invasion of grassland: environmental and biotic effects influencing seedling emergence and establishment. Oecologia, 103(2): 214–223.

Olson DM, Dinerstein E, Wikramanayake ED et al. (2001) Terrestrial ecoregions of the world: a new map of life on earth. Bioscience 51(11): 933-938.

Olsson EG and Ouattara S (2013) Opportunities and challenges to capturing the multiple potential benefits of REDD+ in a traditional transnational savannah-woodland region in West Africa. Ambio 42(3): 309–319.

Parikh J and Reddy S (1997). Sustainable regeneration of degraded lands. New Delhi, Tata McGraw -Hill Publ.

Parr CL, Lehmann CER, Bond WJ et al. (2014) Tropical grassy biomes: misunderstood, neglected, and under threat. Trends in Ecology & Evolution 29(4): 205– 213.

Parr JF (2002) A comparison of heavy liquid floatation and microwave digestion techniques for the extraction of fossil phytoliths from sediments. Review of Palaeobotany and palynology 120(3-4): 315-336.

Patel PP (1997) Ecoregions of Gujarat. Report, Gujarat Ecology Commission, GERI Campus, Vadodara, Gujarat.

Patel Y and Joshi PN (2011). A floristic Inventory in the Banni region of Bhuj Taluka, Kachchh district, Gujarat (India). Indian Forester 137(9):1114-1121.

Patnaik R, Gupta AK, Naidu PD, Yadav RR, Bhattacharyya A and Kumar M (2012) Indian Monsoon Variability at Different Time Scales: Marine and Terrestrial Proxy Records. Proceedings of the Indian National Science Academy 78(3): 535–547.

Peng Y, Xiao J, Nakamura T et al. (2005) Holocene East Asian monsoonal precipitation pattern revealed by grain-size distribution of core sediments of Daihai Lake in Inner Mongolia of north-central China. Earth and Planetary Science Letters 233(3-4): 467-479.

Phadtare NR (2000) Sharp increase in summer monsoon strength 4000–3500 cal yr BP in the central Himalaya of India based on pollen evidence from Alpine peat. Quaternary Research 53(1): 122–129.

Pillai AAS, Anoop A, Sankaran M, Sanyal P, Jha DK and Ratnam J (2017) Mid-late Holocene vegetation response to climatic drivers and biotic disturbances in the Banni grasslands of western India. Palaeogeography, Palaeoclimatology, Palaeoecology 485: 869-878.

Piperno DR (2001) A comprehensive guide for archaeologists and paleoecologists. New York: Oxford: Altamira press, A division of Rowman & Littlefield Publishers, Inc.

Piperno, D.R. 2006. Phytoliths: A comprehensive guide for archaeologisrs and paleoecologists.Oxford: AltaMira Press, A division of Rowman & Littlefield Publishers, Inc.

Ponton C, Giosan L, Eglinton TI, Fuller DQ, Johnson JE, Kumar P and Collett TS (2012). Holocene aridification of India. Geophysical Research Letters, 39(3).

Prasad S, Anoop A, Riedel N et al. (2014a). Prolonged monsoon droughts and links to Indo-Pacific warm pool: A Holocene record from Lonar Lake, central India. Earth and Planetary Science Letters 391: 171–182.

Prasad S and Enzel Y (2006) Holocene paleoclimates of India. Quaternary research 66(3): 442-453.

Prasad S, Kusumgar S and Gupta SK (1997) A mid to late Holocene record of palaeoclimatic changes from Nal Sarovar: a palaeodesert margin lake in western India. Journal of Quaternary Science 12(2): 153–159.

Prasad V, Farooqui A, Sharma A et al. (2014b). Mid-late Holocene monsoonal variations from mainland Gujarat, India: A multi-proxy study for evaluating climate culture relationship. Palaeogeography, Palaeoclimatology, Palaeoecology 397: 38–51.

Prasad V, Phartiyal B and Sharma A (2007).Evidence of enhanced winter precipitation and the prevalence of a cool and dry climate during the mid to late Holocene in mainland Gujarat, India. The Holocene 17(7):889–896.

Ratnam J, Tomlinson KW, Rasquinha DN and Sankaran M (2016) Savannahs of Asia: antiquity, biogeography, and an uncertain future. Philosophical Transactions of the Royal Society B: Biological Sciences 371(1703): 20150305.

R Core Team (2017). R: A language and environment for statistical computing. R Foundation for Statistical Computing, Vienna, Austria. Version R-3.3.3 [Software]. Available from: https://www.R-project.org/.

Reimer PJ, Bard E, Bayliss A et al. (2013). IntCal13 and Marine13 radiocarbon age calibration curves 0–50,000 years cal BP. Radiocarbon 55(4): 1869–1887.

Rein B, Lückge A, Reinhardt L, Sirocko F, Wolf A and Dullo WC (2005) El Niño variability off Peru during the last 20,000 years. Paleoceanography 20(4): 1–18.

Roques KG, O'Connor TG, Watkinson AR (2001) Dynamics of shrub encroachment in an African savanna: Relative influences of fire, herbivory, rainfall and density dependence. Journal of Applied Ecology 38(2): 268–280.

Roy PD, Nagar YC, Juyal N et al. (2009) Geochemical signatures of Late Holocene paleo-hydrological changes from Phulera and Pokharan saline playas near the eastern and western margins of the Thar Desert, India. Journal of Asian Earth Sciences 34(3): 275–286.

Sala EO, Chapin FS III, Armesto JJ et al. (2000) Global Biodiversity Scenarios for the Year 2100. Science 287(5459): 1770–1774.

Sankaran M, Hanan NP, Scholes RJ et al. (2005) Determinants of woody cover in African savannas. Nature 438: 846-849.

Sankaran M and Ratnam J. (2013) African and Asian Savannas. In: Levin S (ed) Encyclopedia of Biodiversity. 2nd Edition. Amsterdam: Elsevier Press, pp. 58-74.

Schefuß E, Schouten S and Schneider RR (2005) Climate controls on central African hydrology during the past 20,000 years. Nature 437: 1003-1006.

Scott L (1999) Vegetation history and climate in the Savanna biome South Africa since 190,000 ka: a comparison of pollen data from the Tswaing Crate (the Pretoria Saltpan) and Wonderkrater. Quaternary International 57-58: 215–223.

Seddon AWR, Macias-Fauria M and Willis KJ (2015) Climate and abrupt vegetation change in Northern Europe since the last deglaciation. The Holocene 25(1): 25-36.

Selvaraj K, Ram Mohan V and Szefer P (2004) Evaluation of metal contamination in coastal sediments of the Bay of Bengal, India: geochemical and statistical approaches. Marine Pollution Bulletin 49(3):174–185.

Shanahan TM, McKay N, Overpeck JT et al. (2013) Spatial and temporal variability in sedimentological and geochemical properties of sediments from an anoxic crater lake in West Africa: Implications for paleoenvironmental reconstructions. Palaeogeography, Palaeoclimatology, Palaeoecology 374: 96-109.

Shanahan TM, Overpeck JT, Wheeler CW et al. (2006) Paleoclimatic variations in West Africa from a record of late Pleistocene and Holocene lake level stands of Lake Bosumtwi, Ghana. Palaeogeography, Palaeoclimatology, Palaeoecology. 242(3): 287-302.

Shmida A (1985) Biogeography of the desert floras of the world. In: Evenari M, Noy Meir I and Goodall DW(eds) Ecosystems of the World, Vol. 12a. Hot Deserts and Arid Shrublands, Amsterdam: Elsevier, pp. 23-77.

Singh G, Joshi RD, Chopra SK and Singh AB (1974) Late Qauaternary history of vegetation and climate of the Rajasthan desert, India. Philosophical Transactions of the Royal Society of London. Series B. 267(889): 467–501.

Singh M, Sharma M, Tobschall HJ (2005) Weathering of the Ganga alluvial plain, northern India: implications from fluvial geochemistry of the Gomati River. Applied Geochemistry, 20(1), 1-21.

Singh N and Kar A (2001). Characteristics of major soils of Banni mudflat in arid western India and their relationship with topography. Journal of Arid Environments 48(4): 509–520.

Sinha R, Symkatz-Kloss W, Stüben D, Harrison SP, Berner Z and Kramar U (2006) Late Quaternary palaeoclimatic reconstruction from the lacustrine sediments of the Sambhar playa core, Thar Desert margin, India. Palaeogeography Palaeoclimatology Palaeoecology 233: 252–270.

Sprent JI (2009) Legume Nodulation – a global perspective. Chichester :Willey- Blackwell.

Staver AC, Archibald S and Levin S (2011) Tree cover in sub-Saharan Africa: Rainfall and fire constrain forest and savanna as alternative stable states. Ecology 92(5): 1063–1072.

Staubwasser M, Sirocko F, Grootes P and Segl M (2003) Climate change at the 4.2 ka BP termination of the Indus valley civilization and Holocene south Asian monsoon variability. Geophysical Research Letters 30(8):1425.

Strömberg CAE (2004) Using phytolith assemblages to reconstruct the origin and spread of grass-dominated habitats in the great plains of North America during the late Eocene to early Miocene. Palaeogeography, Palaeoclimatology, Palaeoecology 207(3–4): 239–275.

Sun Q, Wang S, Zhou J et al. (2010) Sediment geochemistry of Lake Daihai, north-central China: Implications for catchment weathering and climate change during the Holocene. Journal of Paleolimnology 43(1): 75–87.

Swain AM, Kutzbach JE and Hastenrath S (1983) Estimates of Holocene precipitation for Rajasthan, India, based on pollen and lake level data. Quaternary Research 19(1): 1–17.

Tao J, Chen MT, Xu S (2006). A Holocene environmental record from the southern Yangtze River delta, eastern China. Palaeogeography, Palaeoclimatology, Palaeoecology 230(3-4): 204–229.

Tierney JE, Lewis SC, Cook BI, LeGrande A and Schmidt GA (2011) Model, proxy and isotopic perspectives on the East African Humid Period. Earth and Planetary Science Letters 307(1-3): 103-112.

Twiss PC (1992) Predicted world distribution of C_3 and C_4 grass phytoliths. In: Mulholland, S.C. (ed.) Phytoliths Systematics: Emerging Issues. Advances in Archaeological and Museum Science, vol. 1. New York: Plenum Press, pp. 113–128.

Ulrich J. (2016) TTR: Technical Trading Rules. R package version 0.23-1. Available at: https://CRAN.R-project.org/package=TTR.

Veldman JW. 2016 Clarifying the confusion: old-growth savannahs and tropical ecosystem degradation. Philosophical Transactions of the Royal Society B. 371: 20150306.

Veldman JW, Buisson E, Durigan G et al. (2015) Toward an old-growth concept for grasslands, savannas, and woodlands. Frontiers in Ecology and the Environment 13(3): 154–162.

Verschuren, D., Laird, K.R., Cumming, B.F. (2000). Rainfall and drought in equatorial East Africa during the past 1100 years. Nature 403: 410 – 413.

Verschuren D, Sinninghe Damste JS, Moernaut J et al. (2009) Half-precessional dynamics of monsoon rainfall near the East African Equator. Nature 462: 637-641.

Waller MP, Street-Perrott FA and Wang H (2007) Holocene vegetation history of the Sahel: Pollen, sedimentological and geochemical data from Jikariya Lake, north-eastern Nigeria. Journal of Biogeography 34(9):1575-1590.

Wanner H, Beer J, Bütikofer J et al. (2008) Mid- to Late Holocene climate change: an overview. Quaternary Science Reviews, 27(19-20), 1791–1828.

White F (1983). The vegetation of Africa: a descriptive memoir to accompany the UNESCO/AETFAT/UNSO vegetation map of Africa. Natural Resources Research 20, UNESCO, Paris.

Whitlock C, Dean WE, Fritz SC et al. (2012) Holocene seasonal variability inferred from multiple proxy records from Crevice Lake, Yellowstone National Park, USA. Palaeogeography, Palaeoclimatology, Palaeoecology 331-332: 90-103.

Williams RJ, Duff GA, Bowman DMJS and Cook GD. (1996). Variation in the composition and structure of tropical savannas as a function of rainfall and soil texture along a large-scale climatic gradient in the Northern Territory, Australia. Journal of Biogeography 23(6):747–756.

Willis KJ, Bailey RM, Bhagwat SA and Birks HJB (2010) Biodiversity baselines, thresholds and resilience: Testing predictions and assumptions using palaeoecological data. Trends in Ecology and Evolution 25(10): 583–591.

Zhang J and Liu CL (2002) Riverine Composition and Estuarine Geochemistry of Particulate Metals in China—Weathering Features, Anthropogenic Impact and Chemical Fluxes. Estuarine, Coastal and Shelf Science 54(6): 1051–1070.